Research Article

Bio-based UV-curable urethane acrylate graphene nanocomposites: synthesis and properties

Abbas Madhi[1] · **Behzad Shirkavand Hadavand**[1]

Received: 28 November 2019 / Accepted: 14 March 2020 / Published online: 20 March 2020
© Springer Nature Switzerland AG 2020

Abstract

Regarding the importance of protection of the environment, and because of avoiding usage of long-term degradable resins and polymers, use of new materials with a natural and renewable resource in the synthesis of urethane polymers has recently drawn many interests. In the present research, environmentally friendly and bio-based UV-curable urethane acrylate graphene nanocomposites were prepared with 0, 1, 2 and 3 weight percentages. Characteristics and properties of the synthesized nanocomposites were evaluated by SEM, AFM, DTG, tensile testing machine, and DMTA. Morphology of the nanocomposite coatings and dispersion of graphene nanoplatelets in polymer matrix were evaluated by SEM. AFM images proved reduction of surface roughness of coatings following the increase in nanofiller amount. According to DTG curves and tensile testing studies, the most enhanced thermal stability and improved mechanical properties belonged to the 3 wt% sample. In addition, results of DMTA confirmed that adding graphene nanoplatelets, especially 3 wt%, to the resin matrix led to viscoelastic properties improvement, including increase in T_g and storage modulus, and decrease in loss tangent and loss modulus.

Keywords UV-curable urethane acrylate · Graphene nanoplatelets · Bio-based nanocomposites · Thermal stability · Viscoelastic properties

1 Introduction

Nowadays, in light of the importance of protection of environment, researchers prefer to use environmentally friendly and biodegradable polymers and resins over the contaminants and long-term degradable polymers [1, 2]. Polyurethanes are among widely used polymers with excellent practical features [3, 4]. UV curing is a method to synthesize some kinds of polymer nanocomposites and includes specific benefits such as fast curing in low temperature during a short time, being bio-friendly because of nonuse of volatile organic solvents, and saving of time and energy [5–7]. Urethane acrylates are one of the main UV curable oligomers among different kinds of polyurethanes that have optimal features including stiffness, flexibility, chemical and thermal resistance, and appropriate physical traits [8, 9]. Polymer composites are derived from oil, on the other hand, oil consumption has been increasingly raised recently, so an alternative source should be taken into account. Because of the advancement of natural fibers detection and composite science, some improved new products have been produced from natural renewable matters which are biodegradable and recyclable [10–12]. Regarding the environmental and economic advantages in addition to accessibility, vegetable oils have drawn much attention. Triglyceride oils as one of the main biopolymer resources are derived from castor oil plant, soybean, palm, sunflower seeds, and colza. Each triglyceride molecule consists of three fatty acids and a glycerol [13, 14]. There are active parts in the structure of triglycerides

---

✉ Abbas Madhi, abbas.madhi@semnan.ac.ir | [1]Department of Resin and Additives, Institute for Color Science and Technology, Tehran 1668814811, Iran.

SN Applied Sciences (2020) 2:724 | https://doi.org/10.1007/s42452-020-2527-4

including double bond, allylic carbon, hydroxyl groups, ester groups, and alpha carbons connected to ester groups that are ready to make chemical bonds with various functional groups. The synthesis process of vegetable oil-based polymers is similar to that of oil polymers in which polymer groups could be produced using active regions of triglycerides [15, 16]. The purpose is to obtain a high level of molecular weight and create transverse connections. Plastics, nanocomposites, and vegetable oil-based adhesives are generally used in different affairs such as industries of automobile, military, aerospace, electronics, medical and advanced structures in building [17]. Castor oil is considered as one of the vegetable oils that is used in the production of different polymers, it is regarded as an unsaturated fatty acid and ricinoleic acid resource, too. Polyurethanes have two soft and hard parts that the hard part consists of diisocyanate and the soft part consists of diols or polyols derived from petrochemical materials [6, 18, 19]. Therefore, castor oil as a natural polyol resource including reactive hydroxyl groups could be applied in the synthesis of polyurethanes, hence, in addition to being affordable and biofriendly, use of castor oil in the synthesis of polyurethanes could be regarded as an invaluable alternative for polyols derived from oil [20–23]. There has been recently a wide range of scientific and industrial research on producing and using polymer nanocomposites to improve the polymer properties and increase its usability in different issues [24–26]. Carbon-based nanoparticles such as nanotubes and graphene, as reinforcer of polymeric materials, are of special status. Using of graphene nanosheets in polymer nanocomposites is proper in comparison with carbon nanotubes, because the production of graphene is more affordable, it lacks some restrictions such as the desire to agglomeration with progressing process, and also, high quality of products in large quantity are the results of usage of them [27–29].

Graphene is a two-dimensional monolayer and as thick as a carbon atom [30, 31]. Many factors including kind of used graphene and its built-in features, the way of graphene dispersion in the polymer matrix and its surface interaction, also its network structure in the matrix could affect final properties and application of graphene. Due to the plate structure and unique features, graphene nanoplatelets could be used as a suitable reinforcer to produce kinds of polymer nanocomposites with optimal properties such as being nonpoisonous, high chemical resistance, excellent mechanical properties, electrical and thermal conductivity, thermal stability and better mechanical features [32, 33].

Viscoelastic properties of the polymer coatings such as glass transition temperature, loss tangent, loss modulus and storage modulus as temperature and frequency dependents are evaluated by DMTA. Additionally, using DMTA data, cross-link density of the coatings could be determined. Thermal and mechanical features of nanocomposite coatings are influenced by chemical structure of the polymer chains and cross-link density. Suitable and uniform dispersion of nano fillers over polymer matrix is a factor that improves viscoelastic properties of nanocomposites [34–36].

In this work, at first, bio-based UV-curable urethane acrylate (PUA) graphene nanocomposite coatings (0, 1, 2 and 3 wt%) were synthesized. In the following, surface morphology and topography, thermal resistance, and mechanical and viscoelastic characteristics of the prepared nanocomposites were analyzed.

2 Experimental

2.1 Materials

To prepare UV-curable urethane acrylate graphene nanocomposite coatings, benzophenone, triethanolamine (TEA) and acetone purchased from Germany's Merck Co. were added to the castor oil-based urethane acrylate resin synthesized in the previous work [37]. Graphene nanoplatelets (GNPs) with 99.5% purity and 2-18 nm thickness were bought of US Research Nanomaterials Co. (USA).

2.2 Measurements

In order to characterize GNPs particles, and to evaluate the distribution of GNPs in the resin matrix, also to study the morphology of fracture surface of the samples, scanning electron microscopy (SEM) was used. SEM device, LEO 1455 VP model (Germany) has the capacity to scan the samples with a magnification of 20-50,000 times. To study surface topography of the coatings, atomic force microscope (AFM) is used. Model of the used AFM device was DME, Dual Scope C26 (Denmark). According to DTG curves, using Perkin Elmer Pyris Diamond (USA), thermal stability of the samples was analyzed. The temperature of the samples shifted from 25 to 600 °C by heating rate of 10 °C/min in a nitrogen atmosphere. By universal testing machine Santam (Iran) and according to STM-5, ASTM D2370, the tensile strength of the samples was tested at room temperature. Dynamic mechanical thermal analyzer (DMTA) is a method to study the viscoelastic features of polymers in the modulus range of 10^3–10^6 MPa. This test was conducted by DMTA device, DMA 242 C model, Netzsch Company (Germany).

2.3 Preparation of PUA/G nanocomposites

Figure 1 shows the castor oil-based urethane acrylate (UA) oligomer chemical structure. Prepared urethane acrylate resin was added to 4 separate beakers individually containing GNPs with 0 (blank), 1, 2 and 3 wt%, and 5 mL acetone into beaker. Then, each mixture was dispersed for 20 min by sonicated until GNPs separated easily. Afterwards, 18 g UA resin and 6 g TMPTA as a reactive diluent were added to each beaker to decrease viscosity. Next, each of these mixtures was dispersed by mechanical stirrer for 5 h at speed 1000 rotations per minute. In order to eliminate the solvent, each mixture was placed in a vacuum oven for 30 min. After solvent elimination and before films preparation, 0.7 g benzophenone as a photo-initiator and 0.7 g triethanolamine as a co-initiator were added to each mixture and again the mixtures were dispersed for 20 min. In the next step, the 120 µ thick nanocomposite films were applied by film applicator, these films were evenly exposed to ultraviolet radiation for 90 s. This process was done through an ultraviolet lamp (Hg, 1 kW, 80 w/cm) [28]. Reaction of nanocomposite films continued to the polymerization of double bonds of the UA oligomer group by radical polymerization [29, 32]. Considering GNPs weight amount, the films were coded as PUA/G 0 wt%, PUA/G 1 wt%, PUA/G 2 wt% and PUA/G 3 wt%. Subsequently, characteristics of prepared films were analyzed.

3 Results and discussion

3.1 Morphology of PUA/G films

Quality of dispersion of the graphene nanoplatelets in PUA matrix with different weight percentages was evaluated by SEM micrographs. SEM images relevant to the prepared PUA/G films are shown in Fig. 2. As Fig. 2a–d shows, soft and gray regions are related to the polymer matrix, and the prominent and bright points indicate how GNPs are dispersed in polymer matrix as one could observe a flat PUA/G 0 wt% with no fracture and excessive particle. During the preparation of PUA/G nanocomposites, GNPs are separated from each other by sonication and high-speed magnetic stirrer to prevent the GNPs from aggregation in the polymer matrix. Therefor the GNPs are homogenously dispersed in the polymer matrix. These findings correspond with the results of surface topography (see Sect. 3.2). As a result, PUA/G 3 wt% is recognized as the optimal sample in term of adaptation to the polymer matrix. Pleasant dispersion of the GNPs and interaction between them and polymer matrix result in the improvement of the properties of the nanocomposite films.

3.2 Study of nanocomposites surface

The atomic force microscopy (AFM) was used to assign the surface roughness of PUA/G nanocomposites with different weigh percentages of graphene. Figure 3 shows changes on the surface topography of the nanocomposite coatings caused by adding 0, 1, 2 and 3 wt% GNPs into the PUA matrix. Various parameters of the roughness, measurable using AFM, including, S_a, S_q, and S_z are respectively average roughness, root mean square of the surface, and average of subtraction of 5 peak heights from deepest valleys [38]. The findings are represented in Table 1. As Fig. 3 and Table 1 indicate, adding 1 wt% GNPs to the PUA matrix resulted in more surface roughness in comparison with pure sample (PUA/G 0 wt%). The reason behind this is the GPNs accumulation in some regions of the polymer matrix. However, as GNPs amount increases, roughness reduces and surface of PUA/G 2 wt% and PUA/G 3 wt% becomes smoother than other samples, this is a result of voids filling, non-migration of GNPs to the nanocomposites surfaces and their adaptation to the urethane acrylate chains in the polymer matrix [39].

3.3 Thermogravimetric analysis

The thermal stability of PUA/G nanocomposites with different weight percentages was examined by derivative

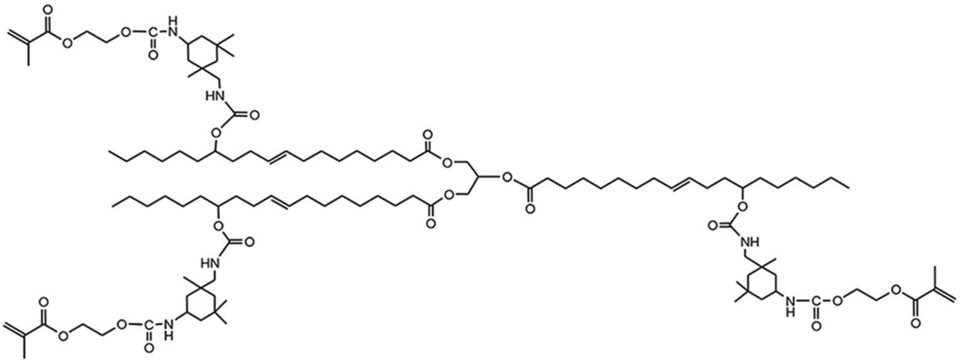

Fig. 1 Chemical structure of the castor oil-based urethane acrylate (UA) oligomer

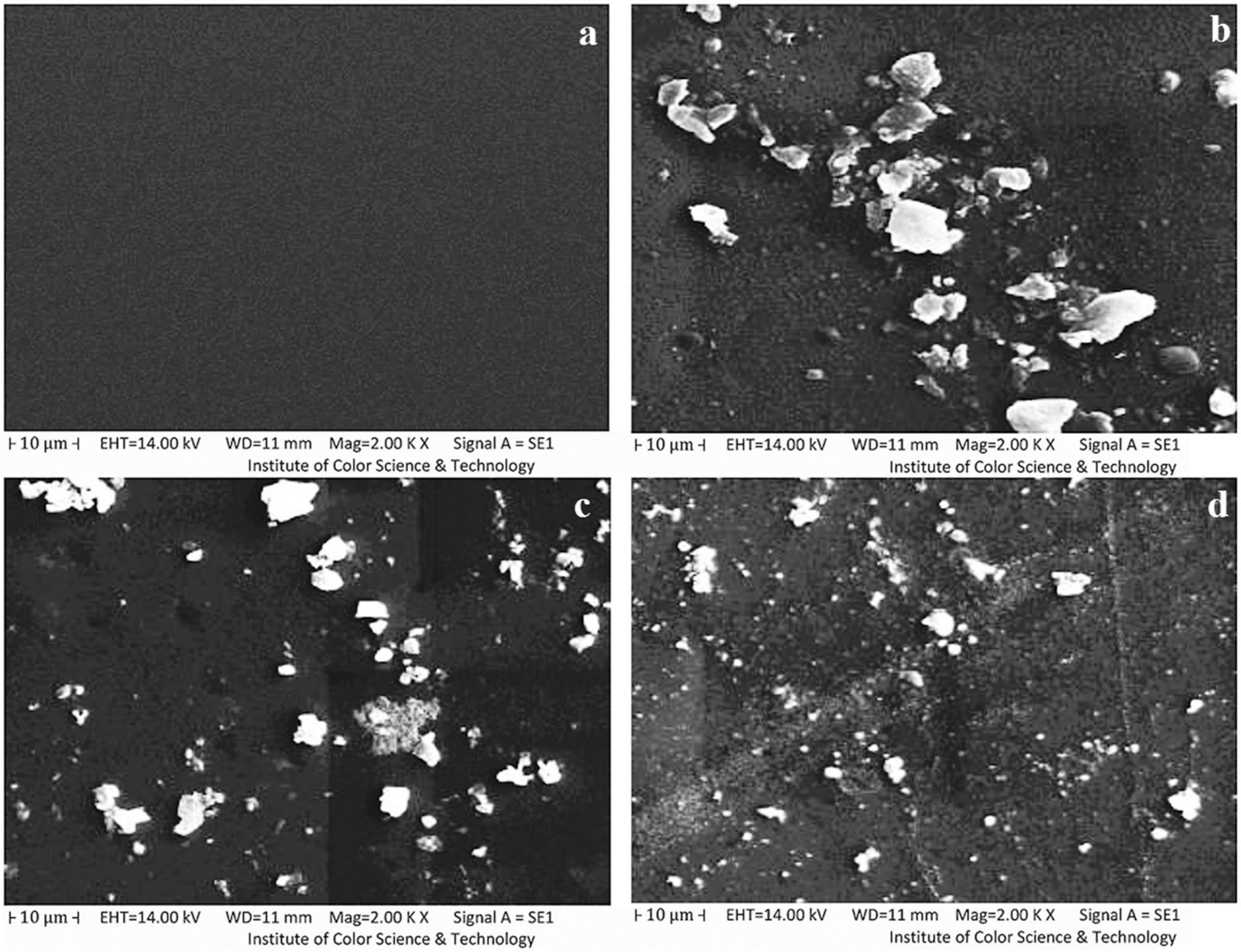
a
b
c
d
10 µm EHT=14.00 kV WD=11 mm Mag=2.00 K X Signal A = SE1
Institute of Color Science & Technology

Fig. 2 SEM images of PUA/G nanocomposites: **a** PUA/G 0 wt%, **b** PUA/G 1 wt%, **c** PUA/G 2 wt% and **d** PUA/G 3 wt%

thermogravimetric (DTG) analysis. Figure 4 shows DTG curves of PUA/G nanocomposites. On the DTG curves, there observed three main peaks appeared at about 100–150 °C that the first was related to solvent, water evaporation and the un-reacted materials. The degradation process of the nanocomposites was accomplished in two steps that the first step was related to the degradation of the polymer chains and nearly 50% took place around 250–350 °C, this range of temperature was regarded as the second main peak. In the second step, complete degradation of the nanocomposites and a rigorous weight loss occurred in the range of 350–500 °C as the third main peak that was related to the separation of the inorganic parts of polymer. Table 2 represents results of DTG of PUA/G nanocomposites (0, 1, 2 and 3 wt%). Increase in temperature led to more weight loss of samples, as Table 2 indicates. According to the results, adding GNPs to the polymer matrix caused thermal stability of the PUA/G nanocomposites to be raised. As the amount of filler increased, the thermal stability increased, too. The maximum thermal stability was observed in PUA/G 3 wt% sample. Two factors of strong chemical interactions between GNPs and polymer matrix, and proper dispersion of GNPs in the polymer matrix are the reasons behind increased thermal stability of the nanocomposites [40].

3.4 Mechanical properties

The strength of a material is measured via tensile properties. In order to have improved mechanical properties, loading nanoparticles into the polymer matrix is a proper technique. Mechanical properties of the PUA/G nanocomposite films with different weight percentages were studied by tensile test. Figure 5 represents the tensile stress–strain curves of PUA/G films.

According to Fig. 5, adding GNPs to the polymer matrix resulted increase in stiffness of samples. Stress values calculated for PUA/G 0 wt%, PUA/G 1 wt%, PUA/G 2 wt%

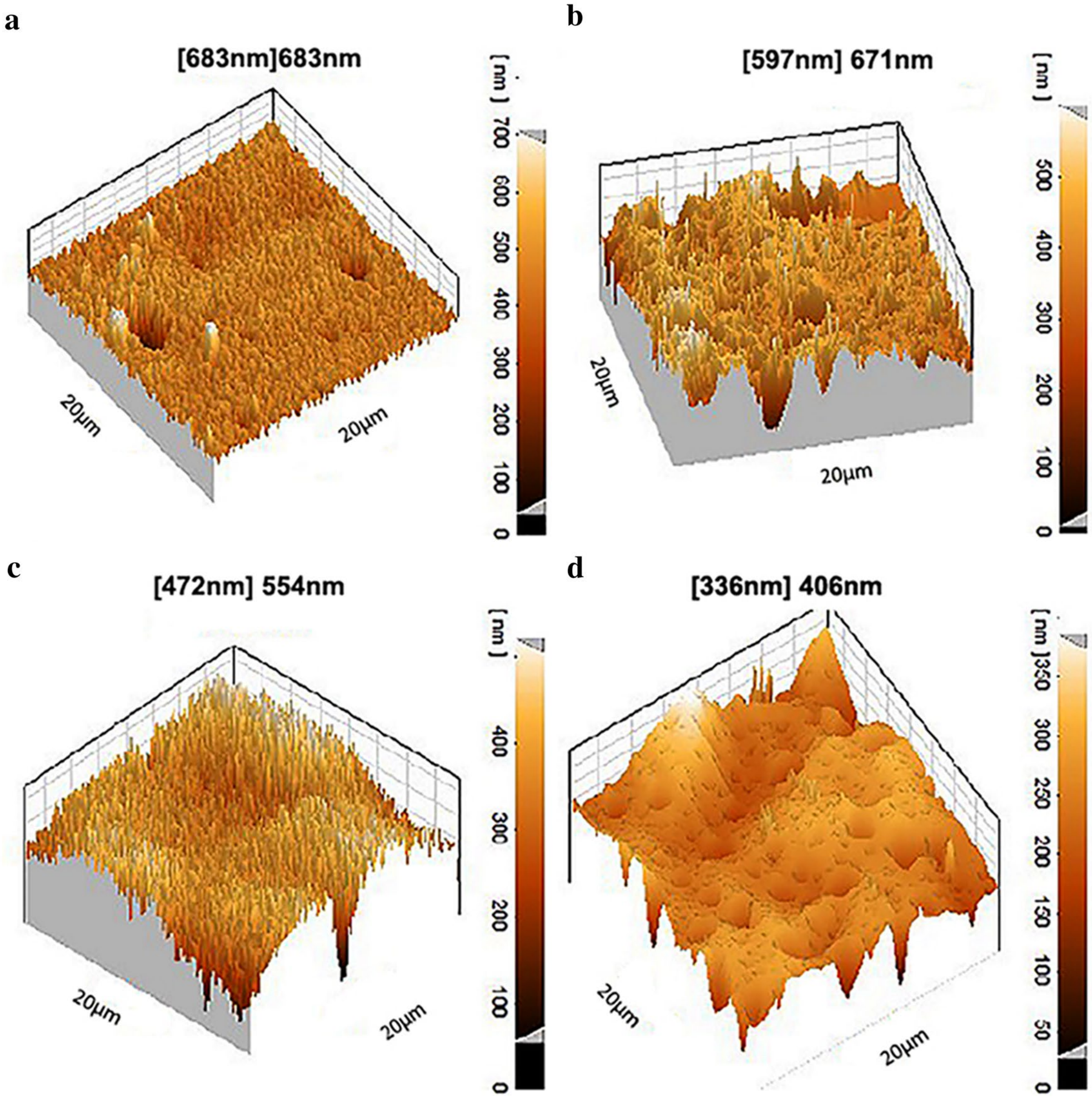

Fig. 3 AFM images of PUA/G nanocomposites: **a** PUA/G 0 wt%, **b** PUA/G 1 wt%, **c** PUA/G 2 wt% and **d** PUA/G 3 wt%

Table 1 Values of roughness parameters for PUA/G nanocomposite coatings

Samples	S_a (nm)	S_q (nm)	S_z (nm)
PUA/G 0 wt%	50.9	71.6	789
PUA/G 1 wt%	74.4	98.1	623
PUA/G 2 wt%	50.2	64.7	492
PUA/G 3 wt%	32.7	44.9	358

and PUA/G 3 wt% were respectively 21.21, 25.60, 27.01 and 29.04 MPa. The reasons behind this are strong interfacial interactions and strong interlayer cohesive energy between graphene nanosheets and polymer matrix [41]. Increasing the amount of graphene increases the amount

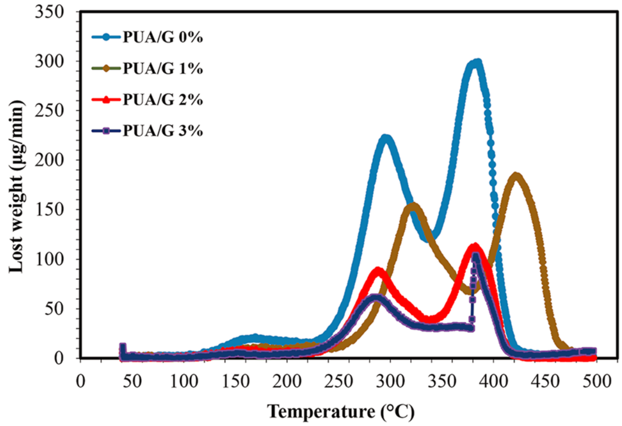

Fig. 4 DTG curves of PUA/G nanocomposites

Table 2 DTG analysis results of PUA/G nanocomposites

Temperature (°C)	Samples			
	PUA/G 0 wt%	PUA/G 1 wt%	PUA/G 2 wt%	PUA/G 3w %
	Lost weight (µg/min)	Lost weight (µg/min)	Lost weight (µg/min)	Lost weight (µg/min)
100	2.47	0.78	0.19	1.2
150	15.4	6.74	6.76	4.48
200	16.2	9.20	6.43	5.26
250	40.9	11.7	20.2	20.4
300	218.8	89.8	74.3	50.4
350	142.6	99.9	44.7	30.7
400	164.6	110.3	66.7	45.7
450	1.60	75.7	0.87	3.21
500	2.12	1.12	2.26	7.54

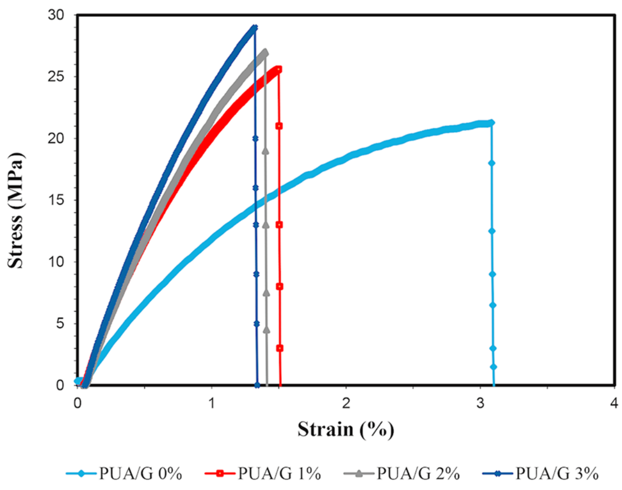

Fig. 5 Stress–strain curves of PUA/G nanocomposites

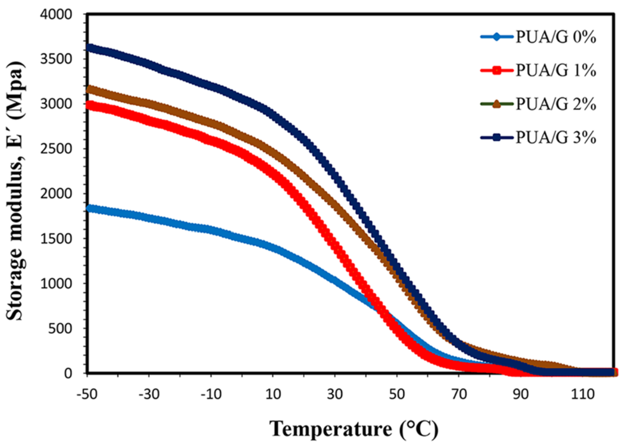

Fig. 6 Temperature dependence curves of the storage modulus (E′) for PUA/G films

of force required due to the increase in crosslink density after curing. Also, due to the increased stiffness, the strain is reduced. Accordingly, the mechanical properties of the PUA/G nanocomposites are improved by the reinforced GNPs.

3.5 Viscoelastic properties

3.5.1 Storage modulus

In order to study the viscoelastic properties of the prepared films, DMTA analysis test was done in a range of temperature. Figure 6 indicates the storage modulus (E′) curves of all the samples that proved value of E′ for all the samples was high in the temperatures lower than − 50 °C, and almost constant up to about 10 °C in a wide range of temperature. As temperature went up, a decrease in E′ of all the samples took place. But in 60–70 °C that is glass transition temperature (T_g), polymer began to become soft, therefore, storage modulus dropped sharply. The effect of GNPs presence on E′ of the coatings was more evident in the temperatures higher than T_g, in a manner difference of E′ value between the samples containing GNPs and the samples without GNPs in the rubbery region was more considerable than the glass region. Increase in E′ in this region showed that GNPs presence optimally led to decrease in movement of polymer network in the rubbery state [39]. Consequently, for the nanocomposites containing higher percentages of graphene there was a higher E′ so that increase in GNPs amount up to 3 wt% caused greatly reinforcement of elasticity features of the polymer and increase in E′, hence, the maximum value of E′ belonged to PUA/G 3 wt%. In a nanocomposite system, some factors such as rate of interaction between inorganic nanoparticles and polymer system, percentage amount of inorganic phase, and quality of dispersion of inorganic nanoparticles are effective. To reach a high storage modulus in nanocomposites, there should be an interfacial adhesiveness between nanoparticles and polymer system through chemical and physical interactions to transfer the mechanical force imposed on the nanocomposite to the nanoparticles with a higher E′ than the polymer system through this interfacial layer. There are many factors affect this interfacial layer that a good dispersion in polymer matrix is the most effective [42, 43].

3.5.2 Loss modulus

Changes of loss modulus (E″) dependent on temperature for PUA/G films with various weight percentages of 0, 1, 2 and 3 are shown in Fig. 7. At the first place, loss modulus of all the samples increased, later it went lower as temperature went up, because the resin matrix showed a resistance against viscoelastic changes, therefore, dispersed nanoparticles wasted energy and loss modulus curve of all the samples shifted to the higher temperatures around 30–50 °C in which the peak height of E″ curve sharply dropped. Compared to the other samples, decrease in loss modulus of 2 wt% and especially 3 wt% samples was remarkable due to the high level of agglomeration of the nanocomposites, therefore, in the system influenced by viscoelastic changes, wasted energy was lowered, because as time passed, nanocomposites began to accumulate, afterward, wasted energy decreased [44]. According to the results, by adding GNPs to the resin matrix, thermal stability and viscoelastic characteristics of the PUA/G films improved considerably.

With respect to higher thermal resistance of the inorganic materials in comparison with organic materials because of the molecular and crystal structure, one could expect noticeable thermal resistance increase.

3.5.3 Loss tangent

Figure 8 shows the curve of loss tangent (tanδ) for PUA/G films. For the 0 and 1 wt% samples, at about 60–70 °C, the peak of tan δ curve first was seen in its highest level, then as temperature rose, it went down. Tanδ curve for the samples 2 and 3 wt% shifted to the temperatures above 70 °C. Meanwhile, the peak became wider than before, also its height declined. For the tanδ curve of 3 wt% sample, the peak was recorded in the lowest height at about 70 °C. Therefore, homogenous dispersion of the GNPs and their chemical and physical interactions with polymer chains caused a better elastic response of the materials.

T_g is considered as one of the main characteristics of the polymers for the study of the polymers mechanical features. The glass transition temperature could be determined using peak of the tanδ curve. Polymers appeared to be hard (glassy) in the temperatures lower than T_g and soft (rubbery) in the temperatures higher than T_g. Enhancement of temperature caused the free volume of the materials to be increased providing for sliding and movement of polymer chains. Above T_g, polymer started to melt. Then one could conclude with increase in GNPs amount, T_g of the coatings goes on the increase, the reason is limitation of movement of polymer chains by inorganic hard phase of GNPs. Accordingly, more thermal energy is necessary in order to achieve T_g [45, 46]. In other words, adding 3 wt% GNPs makes free spaces of the polymer matrix fill that this leads to the increase in mechanical resistance and the stiffness of polymer, hence, T_g goes higher.

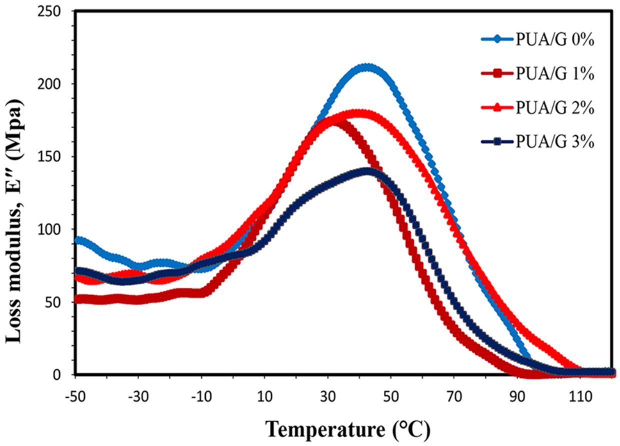

Fig. 7 Temperature dependence curves of the loss modulus (E″) for PUA/G films

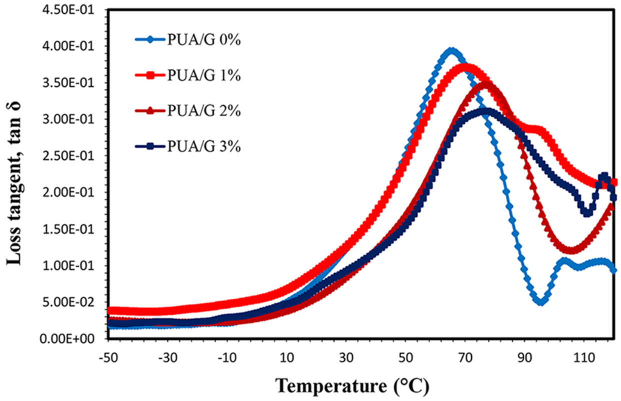

Fig. 8 Temperature dependence curves of the loss tangent (tanδ) for PUA/G films

Table 3 Variations of cross-link density in PUA/G films

Samples	T_g (°C)	E′ (MPa)	Crosslink density (mol/m^3)
PUA/G 0 wt%	65.6	110	13,031
PUA/G 1 wt%	68.3	140	16,453
PUA/G 2 wt%	68.8	256	30,043
PUA/G 3 wt%	78.3	264	30,144

3.5.4 Cross-link density

DMTA data are used for calculating the cross-link density of PUA/G nanocomposite films. Cross-link density of synthesized PUA/G nanocomposites is calculated by Eq. 1 [47, 48].

$$\nu_e = \frac{E'}{3RT} \tag{1}$$

where ν_e, E′, R, T are cross-link density, storage modulus, universal gas constant, and absolute temperature respectively. The obtained results are summarized in Table 3. As results showed, adding GNPs into the polymer matrix caused an increase in cross-link density of samples. Given the mentioned reasons, the increase in storage modulus, and Van der Waals intermolecular forces between organic and inorganic phases were caused by adding more GNPs into the polymer matrix [38, 49]. Therefore, the most value of cross-link density pertained to the PUA/G 3 wt% sample.

4 Conclusion

In the present research, firstly, UV-curable PUA/G nanocomposite coatings (0, 1, 2 and 3 wt%) were produced via ultraviolet irradiation. In the next step, to study the dispersion of GNPs, morphology and surface roughness of the nanocomposites were analyzed by SEM images. SEM micrographs confirmed GNPs were homogenously dispersed in the resin matrix. AFM images proved a remarkable reduction in the surface roughness of 2 and 3 wt% samples by adding GNPs to the resin matrix. The loading of GNPs into the PUA matrix led to improvement in the mechanical properties. DMTA test indicated that loading 3 wt% GNPs into polymer matrix led to note worthy improvement of viscoelastic properties of the prepared nanocomposites. Based on the findings of DMTA data, cross-link density of the synthesized nanocomposites increased. Accordingly, production of affordable and bio-based nanocomposites to consume in various industries using renewable resources can be considered as a realizable plan.

Compliance with ethical standards

Conflict of interest The authors declare that they have no conflict of interest.

References

1. Chen S, Ma C, Zhang G (2017) Biodegradable polymer as controlled release system of organic antifoulant to prevent marine biofouling. Prog Org Coat 104:58–63
2. Dang XG, Yuan HC, Shan ZH (2018) An eco-friendly material based on graft copolymer of gelatin extracted from leather solid waste for potential application in chemical sand-fixation. J Clean Prod 188:416–424
3. Das S, Pandey P, Mohanty S, Nayak SK (2017) Investigation into the influence of UV aging on green polyurethane/nanosilica composite coatings based on transesterified castor oil and palm oil isocyanate. J Inorg Organomet Polym 27:641–657
4. Lee HS, Han CH, Sung YM, Sekhon SS et al (2011) Gel electrolyte based on UV-cured polyurethane for dye-sensitized solar cells. Curr Appl Phys 11:158–162
5. İlgün K, Oktay B, Apohan NK (2018) Methacrylate functionalized MWCNTs/PDMS-polyurethane methacrylate UV-curable nanocomposites. J Inorg Organomet Polym Mater 28:1235–1245
6. Rashmi BJ, Rusu D, Prashantha K et al (2013) Development of water-blown bio-based thermoplastic polyurethane foams using bio-derived chain extender. J Appl Polym Sci 128:292–303
7. Yuan Y, Chen M, Zhou Q, Liu R (2019) Synthesis and properties of UV-curable cardanol-based acrylate oligomers with cyclotriphosphazene core. J Coat Technol Res 16:179–188
8. Najafi F, Bakhshandeh E, Shirkavand Hadavand B, Saeb MR (2014) Toward UV-curable urethane acrylate/silica hybrid coatings: introducing urethane methacrylate trimethoxysilane (UAMS) as organic–inorganic coupling agent. Prog Org Coat 77:1957–1965
9. Farzad H, Najafi F, Bengisu M, Yilmaz E, Shirkavand Hadavand B (2013) Synthesis and characterization of aliphatic tri-functional oligomeric urethane methacrylate used for UV-curable aluminum pigmented coatings. J Macromol Sci Part A Pure Appl Chem 50:504–512
10. Salmiah I, Azizan A, Nor Sabirin M (2015) Characterization of novel castor oil-based polyurethane polymer electrolytes. Polymers 7:747–759
11. Meier MAR, Metzgerb JO, Schubert US (2007) Plant oil renewable resources as green alternatives in polymer science. Chem Soc Rev 36:1788–1802
12. Baştürk E, İnan T, Güngör A (2013) Flame retardant UV-curable acrylated epoxidized soybean oil based organic-inorganic hybrid coating. Prog Org Coat 76:985–992
13. Kasetaite S, Jolita Ostrauskaite J, Grazuleviciene V et al (2017) Biodegradable glycerol-based polymeric composites filled with industrial waste materials. J Compos Mater 51:4029–4039
14. Corma A, Sara I, Alexandra V (2007) Chemical routes for the transformation of biomass into chemicals. Chem Rev 107:2411–2502
15. Panda SS, Samal SK, Mohanty S et al (2017) Characterization, and properties of castor oil-based flexible polyurethane/Cloisite 30B nanocomposites foam. J Compos Mater 52:531–542

16. Cangemi JM, Neto SC, Chierice GO et al (2016) Study of the biodegradation of a polymer derived from castor oil by scanning electron microscopy, thermogravimetry and infrared spectroscopy. Polímeros Ciência Tecnol 16:129–135
17. Mosiewicki MA, Dell'Arciprete GA, Aranguren MI et al (2009) Polyurethane foams obtained from castor oil-based polyol and filled with wood flour. J Compos Mater 43:3057–3072
18. Panda SS, Panda BP, Mohanty S et al (2017) Synthesis and properties of castor oil-based waterborne polyurethane cloisite 30B nanocomposite coatings. J Coat Technol Res 14:377–394
19. Alaa MA, Yusoh K, Hasany SF (2015) Synthesis and characterization of polyurethane–organoclay nanocomposites based on renewable castor oil polyols. Polym Bull 72:1–17
20. Achaby ME, Qaiss A (2013) Processing and properties of polyethylene reinforced by graphene nanosheets and carbon nanotubes. Mater Des 44:81–89
21. Galpaya D, Wang M, Liu M, Motta N, Waclawik E, Yan C (2012) Recent advances in fabrication and characterization of graphene-polymer nanocomposites. Graphene 1:30–49
22. Gurunathan T, Mohanty S, Nayak SK (2015) Isocyanate terminated castor oil-based polyurethane prepolymer: synthesis and characterization. Prog Org Coat 80:39–48
23. Ogunniyi DS (2006) Castor oil: a vital industrial raw material. Bioresour Technol 97:1086–1091
24. Shindume LH, Zhao Z, Wang N et al (2019) Enhanced photocatalytic activity of B, N-codoped TiO_2 by a new molten nitrate process. J Nanosci Nanotechnol 19:839–949
25. Azemati AA, Khorasanizadeh H, Shirkavand Hadavand B et al (2017) Study on radiation properties of polyurethane/nano zirconium oxide nanocomposite coatings. Mater Sci Forum 894:109–112
26. Tian J, Shao Q, Zhao J et al (2019) Microwave solvothermal carboxymethyl chitosan templated synthesis of TiO2/ZrO2 composites toward enhanced photocatalytic degradation of Rhodamine B. J Colloid Interface Sci 541:18–29
27. Martin- Gallego M, Bernal MM, Hernandez M, Verdejo R, Lopez-Manchado MA (2013) Comparison of filler percolation and mechanical properties in graphene and carbon nanotubes filled epoxy nanocomposites. Eur Polym J 49:1347–1353
28. Yuan B, Bao C, Song L, Hong N, Liew KM, Hu Y (2014) Preparation of functionalized graphene oxide/polypropylene nanocomposite with significantly improved thermal stability and studies on the crystallization behavior and mechanical properties. Chem Eng J 237:411–420
29. Haghighat F, Mokhtary M (2017) Preparation and characterization of polyvinylpyrrolidone/magnetite decorated carboxylic acid functionalized multi-walled carbon nanotube (PVP/MWCNT-Fe3O4) nanocomposite. J Inorg Organomet Polym Mater 27:779–787
30. Yu B, Wang X, Xing W, Yang H, Song L, Hu Y (2013) UV-curable functionalized graphene oxide/polyurethane acrylate nanocomposite coatings with enhanced thermal stability and mechanical properties. Ind Eng Chem Res 51:14629–14636
31. Wang X, Xing W, Song L, Yu B, Hu Y, Heng Yeoh G (2013) Preparation of UV-curable functionalized graphene/polyurethane acrylate nanocomposite with enhanced thermal and mechanical behaviors. React Funct Polym 73:854–858
32. Miller SG, Bauer JL, Maryanski MJ, Heimann PJ, Barlow JP, Gosau JM, Allred RE (2010) Characterization of epoxy functionalized graphite nanoparticles and the physical properties of epoxy matrix nanocomposites. Compos Sci Technol 70:1120–1125
33. Xu Z, Gao C (2010) In situ polymerization approach to graphene-reinforced nylon-6 composites. Macromolecules 43:6716–6723
34. Madhi A, Shirkavand Hadavand B, Amoozadeh A (2018) UV-curable urethane acrylate zirconium oxide nanocomposites. Synthesis, study on viscoelastic properties and thermal behavior. J Compos Mater 52:2973–2982
35. Shirkavand Hadavand B, Najafi F, Saeb MR et al (2017) Hyperbranched polyesters urethane acrylate resin: a study on synthesis parameters and viscoelastic properties. High Perform Polym 29:651–662
36. Mohtadizadeh F, Zohuriaan-Mehr MJ, Shirkavand Hadavand B, Dehghan A (2015) Tetra-functional epoxy-acrylate as crosslinker for UV curable resins: synthesis, spectral, and thermo-mechanical studies. Prog Org Coat 89:231–239
37. Madhi A, Hadavand BS (2019) Eco-friendly castor oil-based UV-curable urethane acrylate zinc oxide nanocomposites: synthesis and viscoelastic behavior. J Compos Mater 54:101–110
38. Shirkavand Hadavand B, Pishvaei M, Hosseininiasari M (2019) The role of nanoclay on surface roughness and characteristics of epoxy polysulfide nanocomposite. Prog Org Coat 131:60–66
39. Oleivi JK, Anaee R, Radhi SH (2018) Roughness, wear and thermal analysis of UHMWPE nanocomposites as acetabular cup in HIP joint replacement. J Mech Prod Eng Res Dev 8:855–864
40. Madhi A, Shirkavand Hadavand B, Amoozadeh A (2018) Synthesis, characterization and study on thermal stability, mechanical properties and thermal conductivity of UV-curable urethane acrylate clay (MMT) nanocomposites. J Appl Chem 12:91–98
41. Deshmukh K, Basheer Ahamed M, Sankaran S, Khadheer Pasha SK, Sadasivuni KK, Ponnamma D, Al-Ali AlMaad M (2018) Studies on the mechanical, morphological and electrical properties of highly dispersible graphene oxide reinforced polypyrrole and polyvinylalcohol blend composites. Mater Today 5:8744–8752
42. Shirkavand Hadavand B, Hosseini H (2017) Investigation of viscoelastic properties and thermal behavior of photocurable epoxy acrylate nanocomposites. J Sci Eng Compos Mater 24:691–697
43. Rafiee MA, Rafiee J, Wang Z, Song H et al (2009) Enhanced mechanical properties of nanocomposites at Low graphene content. ACS Nano 3:3884–3890
44. Hassan A, Rahman NA, Yahya R (2011) Extrusion and injection-molding of glass fiber/MAPP/polypropylene: effect of coupling agent on DSC, DMA and mechanical properties. J Reinf Plast Compos 30:1223–1232
45. Madhi A, Shirkavand Hadavand B, Amoozadeh A (2017) Thermal conductivity and viscoelastic properties of UV-curable urethane acrylate reinforced with modified Al2O3 nanoparticles. Prog Color Color Coat 10:193–204
46. Samal SK, Mohanty S, Nayak SK (2009) Polypropylene bamboo/glass fiber hybrid composites: fabrication andanalysis of mechanical, morphological, thermal, and dynamic mechanical behavior. J Reinf Plast Compos 28:2729–2748
47. Song L, Ye Q, Ge X, Misra A, Laurence JS, Berrie CL, Spencer P (2014) Synthesis and evaluation of novel dental monomer with branched carboxyl acid group. J Biomed Mater Res, Part B 102:1473–1484
48. Krongauz VV (2010) Diffusion in polymers on crosslink density Eringappoarch mechanism. J Them Anal Calorim 102:435–445
49. Mohammadian J, Shirkavand Hadavand B, Khajenoori S (2018) Synthesis and investigation on viscoelastic properties of urethane acrylate-polyaniline. Prog Color Color Coat 11:241–252

Publisher's Note Springer Nature remains neutral with regard to jurisdictional claims in published maps and institutional affiliations.